INTERACTION OF SEMICONDUCTOR MATERIALS WITH LASER RADIATION AT 10.6 MICROMETERS

R. D. Bates, Jr., et al

Army Electronics Command
Fort Monmouth, New Jersey

December 1972

AD

Research and Development Technical Report
ECOM-4059

INTERACTION OF SEMICONDUCTOR MATERIALS WITH LASER RADIATION AT 10.6 MICROMETERS

R. D. Bates, Jr.
C. F. Cook, Jr.
J. R. Shappirio
R. S. Rohde
J. P. Mahoney

December 1972

ECOM
UNITED STATES ARMY ELECTRONICS COMMAND · FORT MONMOUTH, N.J.

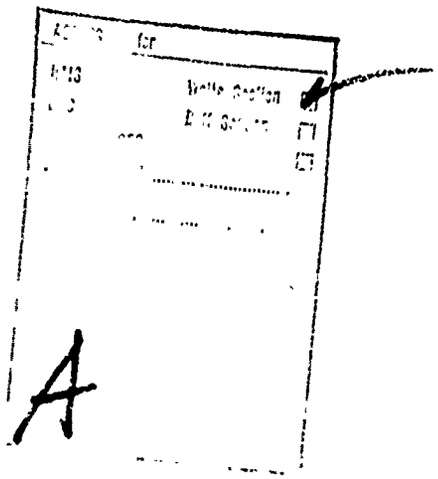

NOTICES

Disclaimers

The findings in this report are not to be construed as an official Department of the Army position, unless so designated by other authorized documents.

The citation of trade names and names of manufacturers in this report is not to be construed as official Government indorsement or approval of commercial products or services referenced herein.

Disposition

Destroy this report when it is no longer needed. Do not return it to the originator.

Specific Control Symbol OSD-1366

TECHNICAL REPORT ECOM-4059

INTERACTION OF SEMICONDUCTOR MATERIALS WITH LASER RADIATION AT 10.6 MICROMETERS

by

R. D. Bates, Jr., C. F. Cook, Jr., J. R. Shappirio

Electronic Materials Research Technical Area
US Army Electronics Technology and Devices Laboratory

R. S. Rohde and J. P. Mahoney

Electro-optics Technical Area
US Army Combat Surveillance and Target Acquisition Laboratory

DA Work Unit Number 1T0 61102 B11A 01 144

December 1972

U. S. ARMY ELECTRONICS COMMAND
FORT MONMOUTH, NEW JERSEY 07703

I

ABSTRACT

Initial experiments characterizing the nature and mechanisms of electronic materials failure when irradiated by CW 10.6 μm CO_2 laser light have been performed. The selective application of such techniques as optical microscopy, scanning electron microscopy, electron microprobe analysis, x-ray crystallography, spin resonance spectroscopy, and infrared spectroscopy provides a specialized facility for the detailed characterization of the nature of the damage state and the paths which lead to this state. Preliminary results on the changes induced in silicon samples show five distinct phases: 1) thermal etching; 2) stress relief through formation of slip traces and cracks; 3) peak formation; 4) melting; and 5) abrupt surface modification. These detailed results are unique in the study of 10.6 μm laser irradiation of semiconductor materials. The nature of these mechanisms and the possible means of component immunization are discussed. Early steps in the development of a theoretical molecular model for the use of a static absorbing gas as a damage prevention mechanism are given.

UNCLASSIFIED
Security Classification

DOCUMENT CONTROL DATA - R & D

(Security classification of title, body of abstract and indexing annotation must be entered when the overall report is classified)

1. ORIGINATING ACTIVITY (Corporate author)
U.S. Army Electronics Command
Fort Monmouth, New Jersey 07703

2a. REPORT SECURITY CLASSIFICATION
UNCLASSIFIED

2b. GROUP

3. REPORT TITLE
Interaction of Semiconductor Materials with Laser Radiation at 10.6 Micrometers

4. DESCRIPTIVE NOTES (Type of report and inclusive dates)
Technical Report

5. AUTHOR(S) (First name, middle initial, last name)
R.D. Bates, Jr., C.F. Cook, Jr., J.R. Shappiro, R.S. Rohde, and J.P. Mahoney

6. REPORT DATE	7a. TOTAL NO. OF PAGES	7b. NO. OF REFS
December 1972	33	55

8a. CONTRACT OR GRANT NO.	9a. ORIGINATOR'S REPORT NUMBER(S)
b. PROJECT NO. 1T0 61102 B11A	ECOM-4059
c. Task No. -01	9b. OTHER REPORT NO(S) (Any other numbers that may be assigned this report)
d. Work Unit No. -144	

10. DISTRIBUTION STATEMENT
Approved for public release; distribution unlimited.

11. SUPPLEMENTARY NOTES	12. SPONSORING MILITARY ACTIVITY
	US Army Electronics Command Fort Monmouth, New Jersey 07703 AMSEL-TL-E

13. ABSTRACT
Initial experiments characterizing the nature and mechanisms of electronic materials failure when irradiated by CW 10.6 um CO_2 laser light have been performed. The selective application of such techniques as optical microscopy, scanning electron microscopy, electron microprobe analysis, x-ray crystallography, spin resonance spectroscopy, and infrared spectroscopy provides a specialized facility for the detailed characterization of the nature of the damage state and the paths which lead to this state. Preliminary results on the changes induced in silicon samples show five distinct phases: 1) thermal etching; 2) stress relief through formation of slip traces and cracks;3) peak formation; 4) melting; and 5) abrupt surface modification. These detailed results are unique in the study of 10.6 μm laser irradiation of semiconductor materials. The nature of these mechanisms and the possible means of component immunization are discussed. Early steps in the development of a theoretical molecular model for the use of a static absorbing gas as a damage prevention mechanism are given.

DD FORM 1 NOV 65 1473 REPLACES DD FORM 1473, 1 JAN 64, WHICH IS OBSOLETE FOR ARMY USE. (2)

UNCLASSIFIED
Security Classification

II b

Security Classification

14. KEY WORDS	LINK A		LINK B		LINK C	
	ROLE	WT	ROLE	WT	ROLE	WT
Laser Damage						
Semiconductors						
Silicon Thermal Etching						
CO_2 Laser						
Molecular Energy Transfer Microscopy						

UNCLASSIFIED
Security Classification

II A/

CONTENTS

TABLE

FIGURES

INTRODUCTION

Preventing damage to electronic and optic components by laser radiation requires complete description of the initial, intermediate and final states of the material. The detailed mechanism and rate of final state development must be defined. Halting the destruction of the material can be accomplished either by designing materials immune to the mechanism involved or by interrupting the processes which lead to the undesirable final state.

This report describes initial experiments which characterize the results of laser interaction with electronic materials. The coupling of laser expertise with materials characterization facilities provides a specific route for investigation of the failure of electronic components, with the goal of generating the understanding necessary to devise means of protecting the components. Previous studies have localized on failure mechanisms in laser systems components, particularly with lasers operating in the visible and near IR. Most work has failed to investigate the cause and effect nature of the interaction. Experiments concentrating on CO_2 laser interaction with ancillary components neglect detailed characterization of the processes and results involved in the formation of the destructive state.

OUTLINE OF PROGRAM

1. Purpose

The research program is designed to develop in detail the characterization of the nature and mechanism of laser interaction with electronic and optic components. The goal is to generate the necessary physical understanding to devise means of protecting the components.

2. General Plan

a) Search public and limited distribution literature to develop a feeling for past and present activity, with emphasis on developing innovative approaches to problem definition and component immunization rather than simply duplicating or extending past studies.

b) Select representative, scientifically well-defined materials and characterize them before, during, and after being damaged by laser light at 10.6 μm.

c) Examine these materials in detail after interaction with laser radiation of varied intensities and for different time periods.

d) Carry out a time-dependent study of the mechanisms of initiation of damage to determine the time scale for effective action.

e) Determine the feasibility of both permanent and activated protective mechanisms based on theoretical and experimental information obtained.

f) Study the same sample materials using the selected protective measures.

g) Develop and investigate new materials specifically chosen for their immunity to laser damage.

(h) Study militarily functional materials to determine effects on operating characteristics using proposed protective measures.

HISTORICAL SURVEY

Early work in laser materials interaction was limited primarily to specific studies of the rates and mechansims in the lasing medium. As the desired output powers were increased, specifics of the breakdown of the lasing materials became important.[1-4] Detailed studies of damage to glass laser rods dominate the published literature, with a significant contribution coming from the USSR.[5] Studies of the molecular dynamics in gas laser systems became an integral part of the continued development of new and more efficient systems.[6,7] Each new systems development such as TEA,[8] gas dynamic[9] or chemically generated[10] laser media spurred new studies of the laser system itself.

Complementary to the development of newer, more efficient lasing systems was the growth of means to modify, control, and handle the output. Inactive devices such as windows and mirrors showed the rigors of increased requirements, and studies of the effects of laser radiation on ancillary components were initiated. Active elements such as frequency doublers, mode-locking species, passive Q-switches, and optical shutters greatly increased the versatility of the laser system and naturally ushered in a fundamental investigation of the principles of operation, including failure mechanisms. The effect of a propagating laser beam on the medium and vice versa became an important topic of study.[11,12] The mechanistic investigation of the dynamics of the system became the key to new developments.

The present practical uses of the laser already exceed the wildest dreams of the progenitors of the laser era.[13-15] With this new technology comes the necessity for detailed studies of laser-matter interaction, whether deliberate or accidental in nature. This general area has been much less intensively explored than the previous two. The use of lasers to develop chemical changes has been expanding,[16] but the effect on electronic materials has not been thoroughly investigated.

This work is concerned specifically with the interaction of CO_2 laser radiation at 10.6 μm with materials, and the means to inhibit component failure. Previously published work on CO_2 laser damage to materials is alarmingly limited. The effects of CO_2 laser radiation on potential laser window materials have received some attention.[17] Studies have been made of plasma formation on irradiation of thin metal films,[18,19] while reflecting metal films have been investigated as a means of shielding optical components.[20] Two papers have dealt with the damage to semiconductor materials.[21,22] Laser interactions with germanium have demonstrated photon drag effects,[23,24] and stimulated Raman emission has been observed from interaction with semiconductor materials.[25] The field remains virtually virgin for detailed characterization studies of the damage state and the dynamics and mechanisms of damage production.

SELECTION OF MATERIALS

Four typical materials were selected for an initial series of experiments: 1) silicon; 2) a sensor material; 3) an optical component material; and 4) an amorphous semiconductor.

Our work thus far has been devoted to detailed examination of silicon damage, since the careful evaluation of the behavior of an elemental material is required as the foundation for future understanding of multicomponent materials. With this basis the specifics of actual devices will be an extension of the work on simpler substances.

EXPERIMENTAL PROCEDURE

1. Laser Facility

A CW 10.6 μm CO_2 laser constrained to operate on a single line was available for irradiation of samples. The output was focused on the sample by a germanium lens, with a localized power level of 5 kW/cm^2 in a spot of approximately 1 mm^2. A mechanical beam chopper provided square-wave light pulses of a chosen time duration. Initial experiments were performed on samples in air, the sample being supported in a vertical position free from interference by supporting material behind the specimen.

A laser sample chamber was designed and constructed. This provided an accurate means of sample positioning, with the capability of vacuum chamber irradiation or irradiation in a controlled atmosphere. The chamber was equipped with a laser beam entrance window plus several exit windows for monitoring secondary photon emission or performing double beam experiments. Additional parts in the chamber were available for <u>in situ</u> observation of chemical and physical properties of sample materials.

2. Sample Preparation

Two types of silicon materials were used. Set 1 consisted of commercially prepared wafers of 150-[illegible] ohm-cm p-type silicon which had been float zone refined. Samples were 0.2 mm thick with one polished side. Set 2 consisted of silicon wafers cut from a 500-600 ohm-cm boule. Some of these wafers of varying thicknesses were left unpolished, some mechanically polished, and some polished both mechanically and chemically. All sample wafers were cut parallel to the (111) crystallographic plane. Sample surfaces were cleaned before irradiation.

3. Characterization Facility

Several experimental techniques were used on an exploratory basis in an attempt to develop significant standardized methods for the morphological, structural and chemical characterization of laser irradiated materials. The methods which were found to be distinctly beneficial for silicon samples were optical microscopy, scanning electron microscopy, Laue x-ray diffraction, infrared spectroscopy, and electron spin resonance.

The optical microscope detects changes in reflected light intensity, and is most useful for studying small changes in surface relief rather than gross deviations, as only one altitude can be in focus at a given time due to the short depth of focus. Complementing this technique is the scanning electron microscope which provides a much greater depth of field. Observation of secondary electron emission from the surface and near subsurface provides general topographical information as well as specific data concerning areas of varying secondary electron emission characteristics. The Laue x-ray diffraction technique provides data on the crystal symmetry

of the sample. Infrared spectroscopy is used to detect changes in absorption properties of the material principally through changes in chemical composition. Another powerful technique for observation of microscopic chemical composition which could not be used for elemental silicon, yet will provide specific information on future materials is the electron microprobe. Future samples will also be examined by a broad spectrum of additional characterization techniques including electron and x-ray diffraction, nuclear magnetic resonance, mass spectrographic analysis, emission spectroscopy, microindentation hardness, Auger spectroscopy, and thermal analysis. The most useful procedures will be determined for each representative material.

EXPERIMENTAL RESULTS

The first series of irradiation experiments was performed on silicon samples placed at the focal point of the lens. The purpose was to produce observable damage with the CW CO_2 laser at 5 kW/cm^2. Set one samples and polished set two samples shattered into multiple fragments which flew distances of several feet when irradiated near or at the center of the sample. However, other samples irradiated at or near the edge did not show any evidence of catastrophic breaking for exposure periods as long as 5 sec. Samples exposed for 5 sec were heated to a dull red at the end of the exposure period. Surface perturbation observable with unaided eye was produced for samples exposed for as little as 2 sec.

Unpolished samples approximately 0.6 mm thick exposed to CW CO_2 laser radiation for periods as long as 10 sec also glowed red after approximately half the exposure period, but no damage other than the presence of a dark spot in the area of irradiation was observable, though small changes could easily have been masked by the roughness of the surface.

CHARACTERIZATION RESULTS

Figure 1-1 is a light micrograph (LM) showing the damaged region on the polished surface of a silicon sample from set 1 after 2 sec irradiation by a CO_2 laser. The damaged area is circular in shape, approximately 1200 μm in diameter, and consists of three distinct and nearly concentric regions: an outer perimeter band, a more reflective inner band, and a central dark region. Figure 1-2 is a higher magnification view of part of the irradiated region. The perimeter band is about 80 μm wide and consists of an outer margin of trigonally symmetric, interconnected etch pits. The sharp boundaries of the perimeter pits become more rounded and less geometrically defined toward the inner margin, so that the sharp, linear etch-pit edges are less regular, curving ridges in the inner region of the perimeter band. While the outer margin of the perimeter is sharp, the inner margin is gradational into the next zone.

Two features perturb the silicon surface outside the circular damage region. Three sets of parallel slip traces are present at angles of 60° and parallel to the edges of the etch pits of the adjacent perimeter region. In addition, as seen in Fig. 1-1, a crack extends from a point on the lower right-hand part of the perimeter region to the nearest edge of the sample. The crack is irregular and not geometrically controlled.

Inside the outer perimeter the surface appears very similar to the undisturbed sample. Three sets of slip traces in this region are similar in

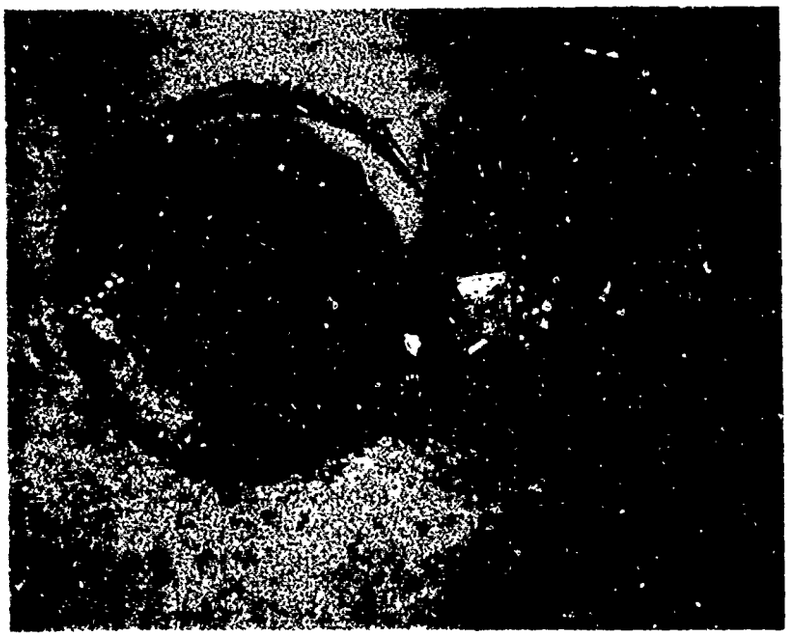

FIGURE I-1. A LIGHT MICROGRAPH AT 56X OF THE IRRADIATED SPOT ON SILICON SAMPLE I.

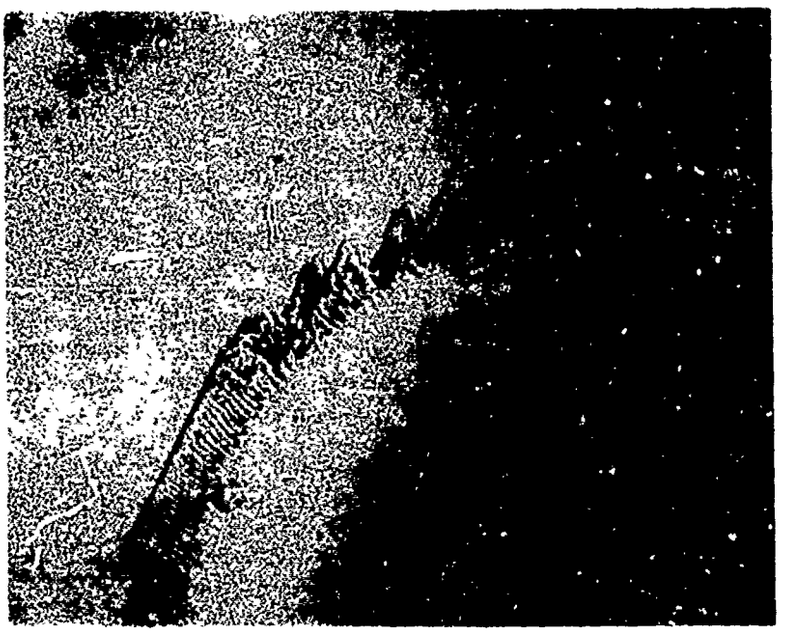

FIGURE I-2. A LIGHT MICROGRAPH AT 135X OF THE SAME SAMPLE.

appearance to those external to the damage region. These lines are not as well defined as those outside, though their direction correlates well with the bulk crystal directions.

The nature of the two inner regions is shown in the scanning electron micrographs (SEM) of Figs. 1-3 and 1-4. The perimeter band which was very distinct in the LMs can still be distinguished. The crack in the sample is readily apparent at the right, but inside the perimeter region it expands to form a deep rounded depression which penetrates through the sample in four places, the largest of which is approximately 160 μm in length. Adjacent to this depression and approximately at the center of the damage spot is a hill, the top of which projects above the plane of the original silicon surface. The surface of the hill is terraced and marked by semi-parallel dark and light bands which are visible primarily due to differences in secondary electron emission. Within the lighter bands, bright lines approximately perpendicular to the bands can be seen. The segments are roughly aligned but broken by the dark bands. At the top of the hill, a nipple-like projection is apparent. (The two bright spots at and near the top of the hill are dirt.)

Figure 1-5 is an SEM of the back side of the same sample at a point corresponding to the perturbed region on the front. Here the original surface was unpolished and appears very rough in the photo. The laser irradiated area is a much smoother surface, though some roughness is still evident scattered through the section. The diameter of the perturbed region on the reverse side is 660 μm. A hollowed-out area appears where the laser broke through the sample, yet even here some evidence of the original sample morphology can still be seen. In the area opposite the protrusion on the front side, a gradual rise is evident, indicating a buildup of material on both sides of the sample at the same point. This is confirmed by the sectioned side view of the same sample shown in Fig. 1-6. This figure also indicates that the buildup of material is not hollow, a possibility which had occurred because of the apparent hole which can be seen on the central raised portion shown in Fig. 1-5. The irregularity surrounding the orifice should also be noted.

Examination of the LM of sample 2 in Fig. 2-1 reinforces most of the observations seen on sample 1. Sample 2 was from set 2, was 0.2 mm thick, and was irradiated for 2 sec. The sample was mechanically polished only, and several scratches which remained can be prominently seen outside the damage spot. Again the three distinct regions of surface perturbation generated by the laser are observable, with the inner regions slightly elliptical. In the lighter region two surface scratches are still evident after irradiation and align with those external to the irradiated region. Slip traces can again be discerned in the lighter band and outside the perturbed region in the lower portion of Fig. 2-1.

The perimeter band of sample 2 has features in common with sample 1, but several differences are apparent. The band itself is considerably wider, ranging from 180 μm to 1000 μm, and is elliptical in shape, but with an extension along a major axis toward the nearest edge. Thermal etching features are more prominent in this sample, primarily because of the width of the zone. At higher magnification the tendency for the sharp edges of the etch pits to become rounded and less linear toward the central dark region is apparent. There is a tendency for the thermally developed etch pits to extend beyond the outer perimeter along original surface scratches.

FIGURE I-3. A SCANNING ELECTRON MICROGRAPH OF SAMPLE I AT 134X and 60 DEGREES.

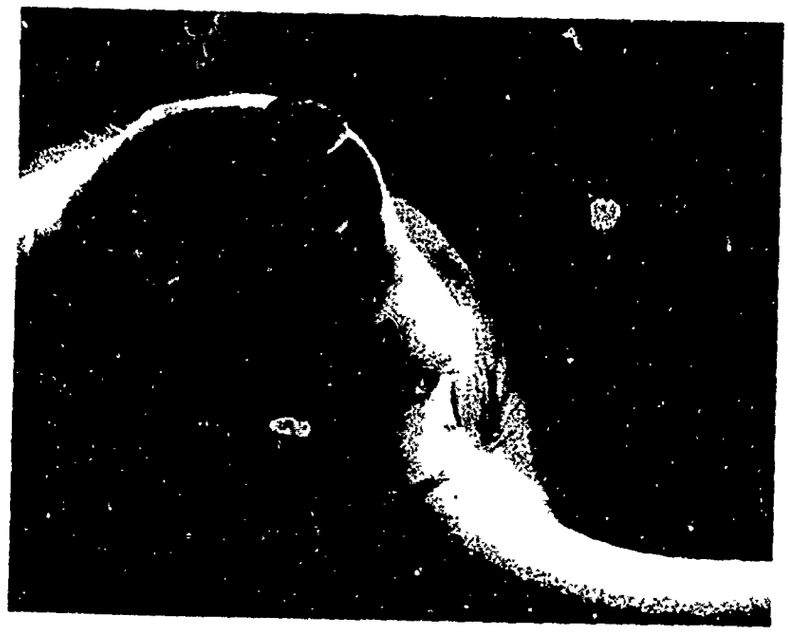

FIGURE I-4. A SCANNING ELECTRON MICROGRAPH AT 335X.

FIGURE I-5 [illegible] PAPH AT 126X
[illegible] SIDE OF
SAM[illegible]

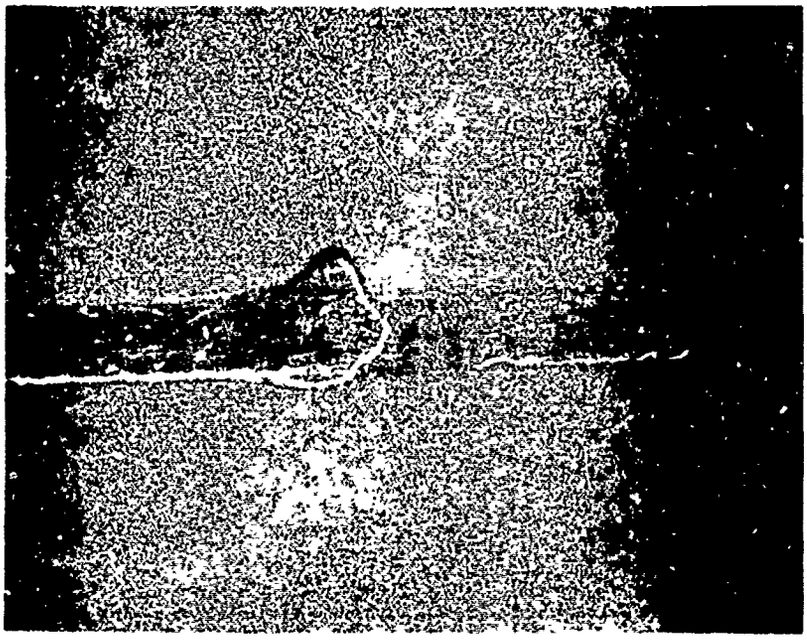

FIGURE [illegible] RAPH OF A

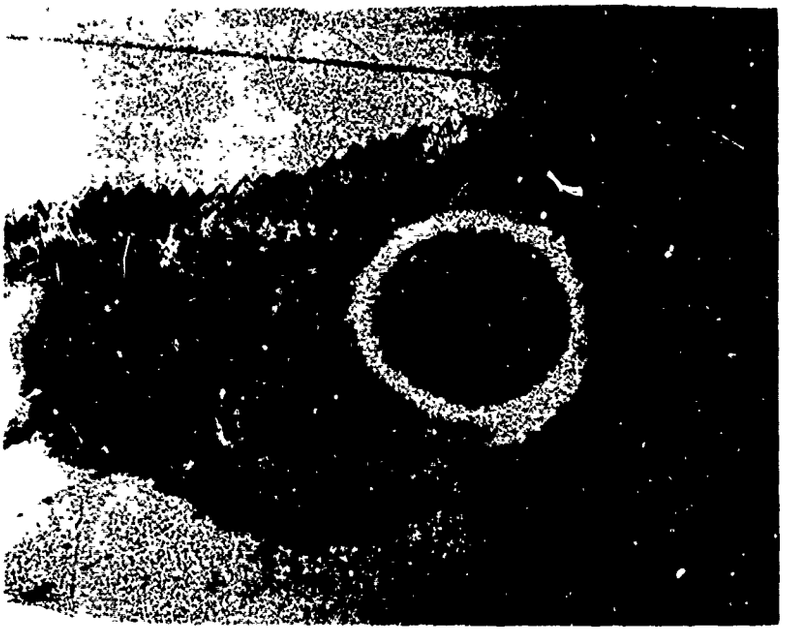

FIGURE 2-1. A LIGI ..OGRAPH AT 56X OF THE IRRADIATED SPOT ..ICON SAMPLE 2.

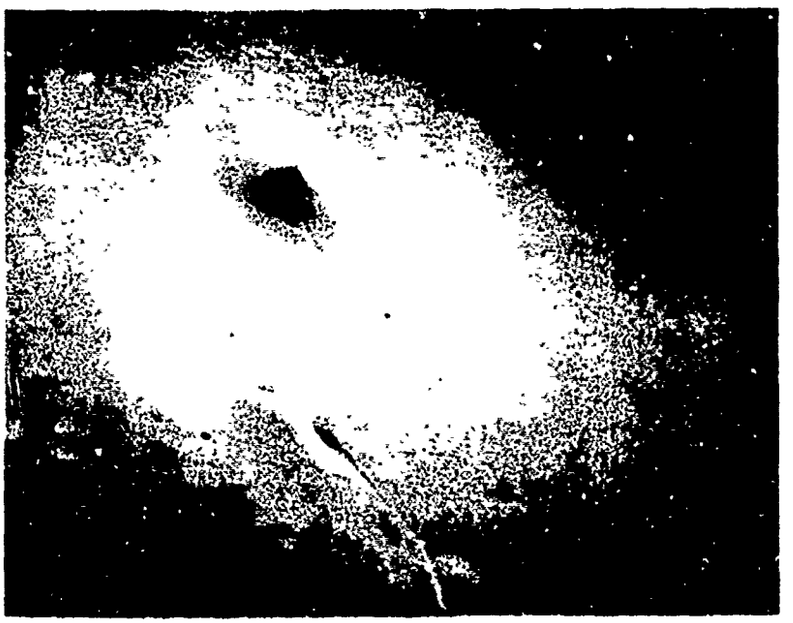

FIGURE 2-2. A SCANNING ELECTRON MICROGRAPH AT 55X AND 60 DEGREES OF THE IRRADIATED SPOT.

Two other regions are noteworthy. A crack can be observed near the left edge of Fig. 2-1. An unetched, crescent-shaped area can be observed in Figs. 2-1 and 2-2, lying between a dark spot at the left of Fig. 2-1 and the two inner regions. The inner edge of this region shows the sharp etching characteristic of the outer edge of the perimeter band, while the outer edge of the region shows the gradation of the etch features seen at the outer edge of the central region.

Figure 2-2 is an SEM showing the entire disturbed region and includes a portion of the nearest edge of the sample. Prominent in the center of the undisturbed area is a large symmetrical peak approximately 40 μm high, which shows a prominent nipple at the top. A magnified view of this feature is shown in Fig. 2-3 and reveals that this peak protrusion stretches 15 μm above the uppermost part of the hill. The hill appears to be terraced by a series of concentric wavelike rings, and a series of dark irregular veins runs down the sides of the hill, apparently emanating from the peak near the point at which the nipple emerges. Figure 2-2 demonstrates that the extended portion of the perimeter area identified in Fig. 2-1 stretches to the nearest edge. The crack is prominent in Fig. 2-2 and terminates in a depression in the thermally etched region. The etched surface is evident only on the left side of the crack near the sample edge. One final feature in Figs. 2-2 and 2-3 is a line of higher electron emission running from just to the right of the crack through the perimeter band, the smooth inner circle, part way up the side of the hill, down the other side and into the perimeter region on the other side. This feature was also identifiable in some regions of Fig. 2-1 as a pre-existing surface scratch. The scratch appears pitted outside the region perturbed by the laser, but no such relief is visible within the central region magnified in Fig. 2-3. This white line is broken and skewed by one of the dark gray veins appearing on the side of the hill, the only position along the line segment length where such a discontinuity is observed.

The discontinuity is again manifest in Fig. 2-4, which is a slightly higher magnification of the side of the peak area shown in Fig. 2-3. Here again the darker veins are evident, though no relief features can be seen for these lines. The concentric rings circumscribing the peak are visible, and they definitely appear as raised and lowered areas. This SEM was taken after the nipple at the top had been removed. The very irregular nature of the remaining crater and the surrounding orifice is strongly contrasted with the smooth topography in the inner two regions. This post-mortem surgery produces a hole quite similar to that observed on the reverse side of sample 1 in Fig. 1-5.

Figure 2-5 is a higher magnification of the termination of the crack inside the etched region. Here the corrugated surface irregularity is evident, and the edges of the fault appear rounded and covered by raised beads similar to the surrounding sample. Outside this perimeter region the interior and the edges of the crack are irregular. Fig. 2-6 is an SEM of the back and side of the sample showing the nature of the crack formed and indicating that it goes entirely through the sample, though not in a vertical plane. Figure 2-7 is an SEM of the reverse side of sample 2. It shows that the back of the sample has an area of higher secondary electron emission similar in shape to the irregular region on the front. In this sample there is no penetration of the samole and the reverse side shows no evidence of surface change observed in the first sample.

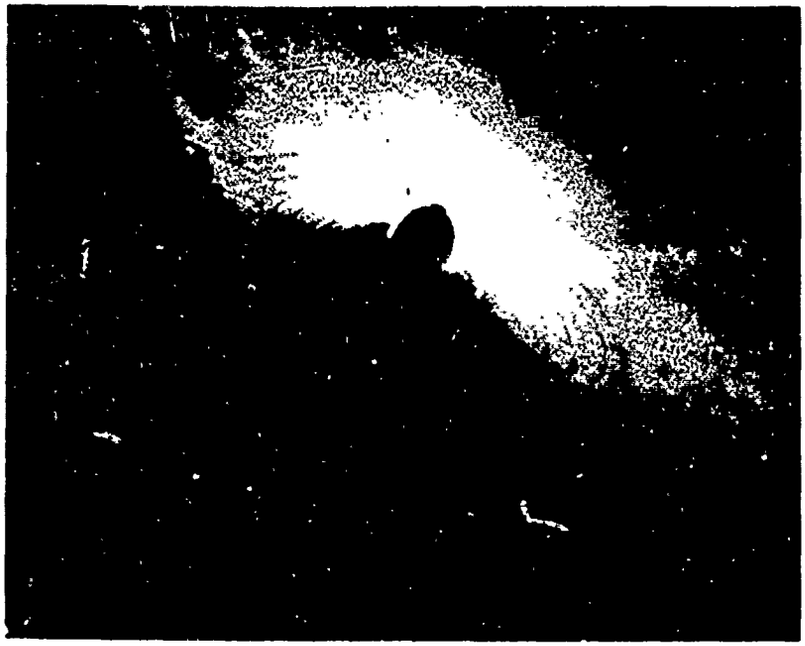

FIGURE 2-3. A SCANNING ELECTRON MICROGRAPH AT 550X AND 60 DEGREES OF THE CENTRAL PEAK ON 2.

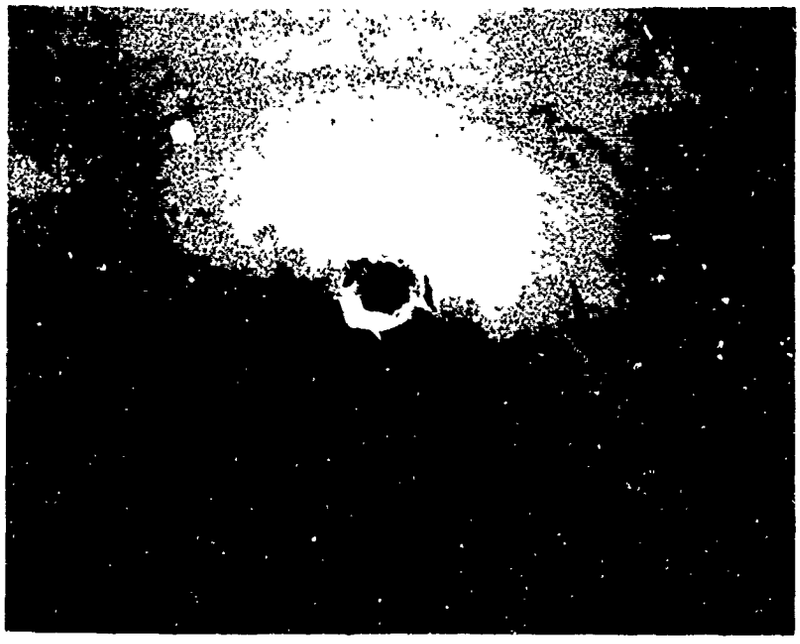

FIGURE 2-4. A SCANNING ELECTRON MICROGRAPH AT 700X AND 30 DEGREES WHICH HAS BEEN ROTATED 100 DEGREES WITH RESPECT TO FIG. 2-3.

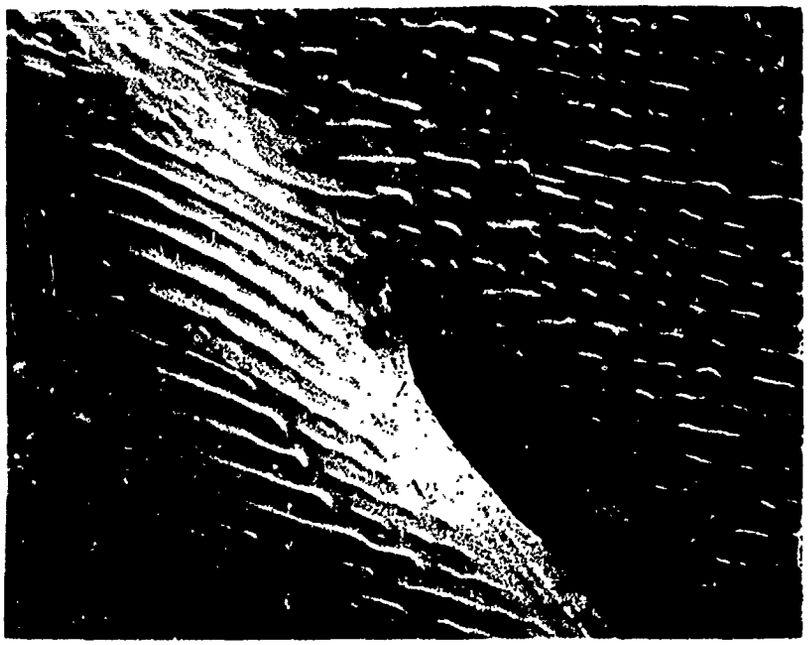

FIGURE 2-5. A SCANNING ELECTRON MICROGRAPH AT 550X AND 60 DEGREES OF THE CRACK TERMINATION ON SAMPLE 2.

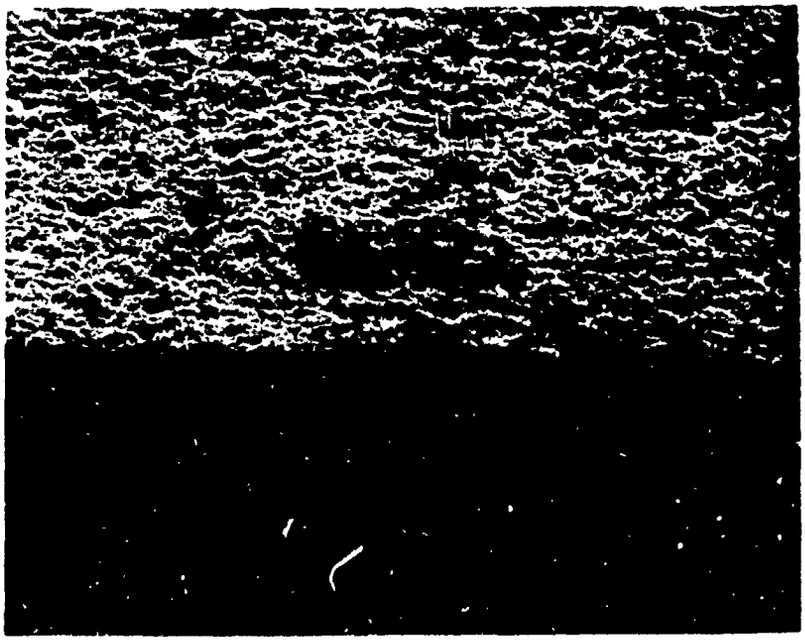

FIGURE 2-6. A SCANNING ELECTRON MICROGRAPH OF THE SIDE AND REVERSE OF SAMPLE 2 AT 124X AND 60 DEGREES.

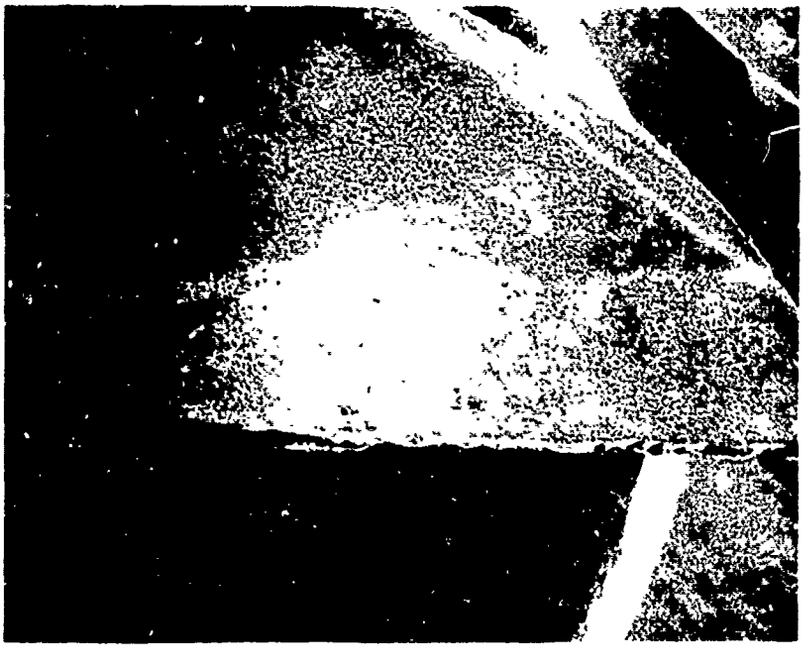

FIGURE 2-7. A SCANNING ELECTRON MICROGRAPH OF SAMPLE TWO REVERSE SIDE AT 13X.

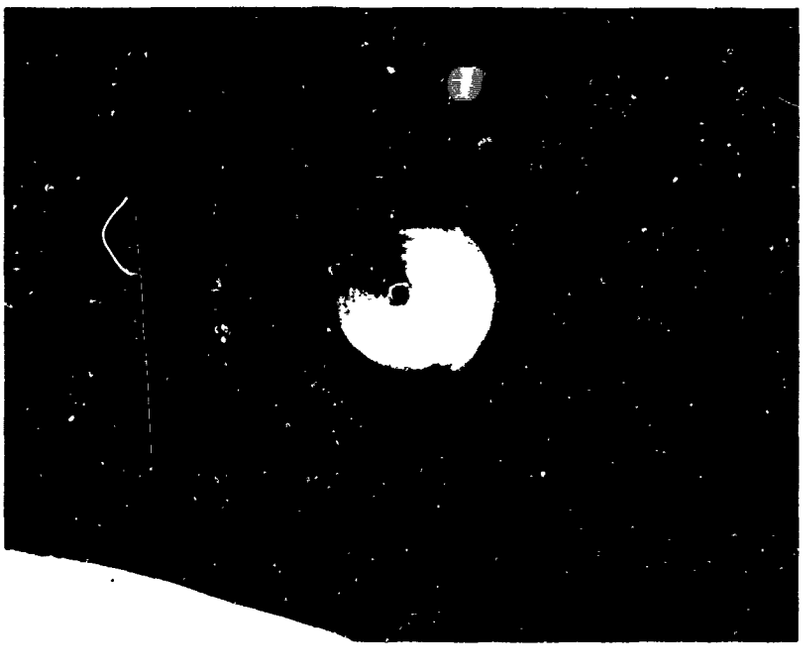

FIGURE 2-8. A DARK FIELD, LIGHT MICROGRAPH AT 210X OF THE CENTRAL PEAK ON SAMPLE 2.

The final figure included for this sample is a dark field LM in which the illuminating light is at an angle to the surface, thus illustrating regions of surface topography not in the surface plane. Figure 2-8 is a top view of the peak strongly demonstrating the concentric rings.

A third sample was from set 2 and received vibratory polishing. This sample was 0.2 mm thick and was irradiated for 2 sec. Figure 3-1 is an LM of the surface region perturbed by laser radiation. Two of the three zones previously observed are again evident, with only the central dark region apparently absent. Trigonal etch pits are much less prominent than in the two previous samples, and are evident here only at the extreme outer margin of the perimeter region. The perimeter region on this sample is dominated by beadlike or wormlike patterns whose distribution shows some evidence of crystallographic control. The central dark region is not prominent, appearing instead as a pimple in the center, with evidence of surrounding slip traces. A portion of a hook-shaped crack to the nearest edge can be seen in Fig. 3-2, an SEM of the irradiated region. The sample shows increased secondary electron emission from the irradiated region.

Sample 4 was from set 1, receiving vibratory and chemical polishing. This wafer was exposed sequentially in two different locations on the polished surface. The first exposure was for 2 sec. During the second exposure, the sample fractured, with the break occurring between the two exposed spots. Figure 4-1 is an LM of the second spot on one of the recovered pieces. Only the outer band is present, with beadlike irregularities prevalent. Triangular etch pits extending into the unperturbed sample are easily distinguished and the slip traces external to the perimeter region are evident. In the lower right corner of Fig. 4-1 along the sample edge, conchoidal fracture patterns are discernible. However, within the irradiated region, the edges seem smoother and more gradual. This observation is reinforced by Fig. 4-2, an SEM of the same region. The dark square in the center of the SEM represents cracked hydrocarbons produced during the electron microscopy. The rugged fracture external to the irradiated area is contrasted with the smooth inner region.

The final sample examined was from set 2 and was irradiated on the unpolished side. The sample fractured after a portion of the 2 sec irradiation period. Figure 5-1 shows a large area of smooth material covering part of the surface and extending in a long, irregular projection away from the sample. This area is sharply contrasted with the rough fracture edge extending to either side. The outer thermally etched region is not discernible on either side of the sample. At the extremity of the projection, the edge is somewhat sharp as if clipped off. A magnified view of a secondary projection, observable in Fig. 5-1 extending to the lower portion of the micrograph, is shown in Fig. 5-2. Here too, darker veins on the projection and surrounding extension surface are evident. The peak of the projection is capped by a nipple-like protrusion. Finally, the lower edge of Fig. 5-2 shows the rough surface of the clipped edge. In the crook shown in Fig. 5-1, a small protuberance of material can be seen, Fig. 5-3 showing a magnification of this area. This point appears very much like the peak in Fig. 2-3. No dark veins surround the projection, though they can be observed on the nipple itself.

The least extensive damage on any of the samples irradiated was observed on a .6 mm thick, unpolished sample from set 1. This was subjected to several laser exposure periods of 10 sec. The sample was heated to a glowing

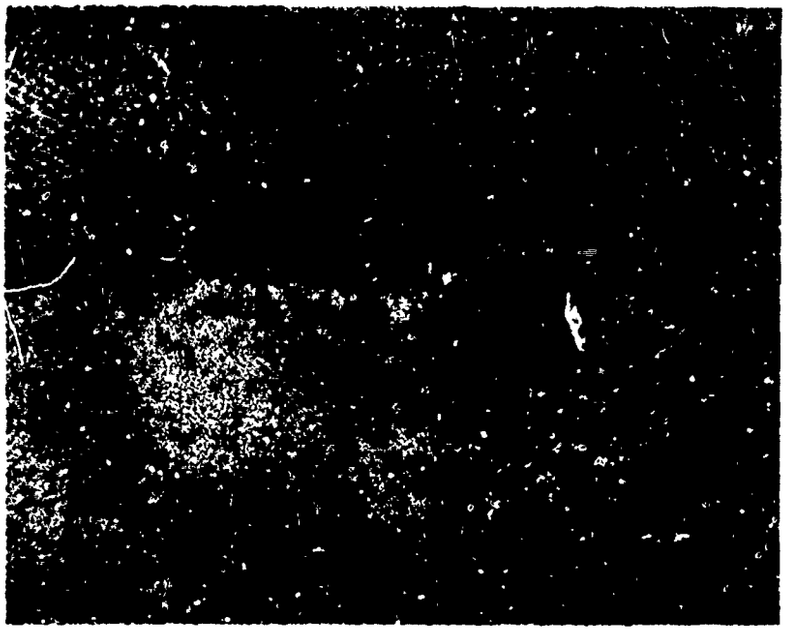

FIGURE 3-1. A LIGHT MICROGRAPH OF THE IRRADIATED REGION OF SAMPLE 3 AT 135X.

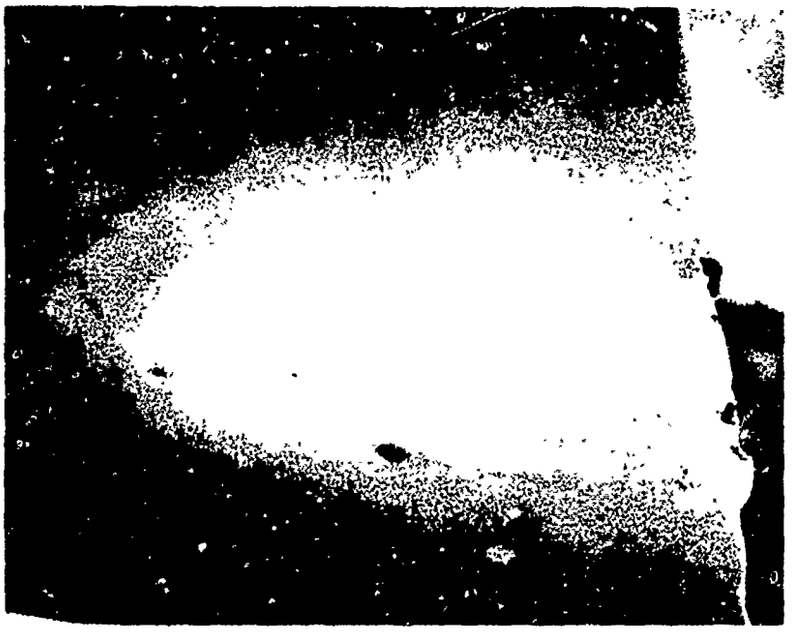

FIGURE 3-2. A SCANNING ELECTRON MICROGRAPH AT 33X AND 60 DEGREES.

FIGURE 4-1. A LIGHT MICROGRAPH AT 135X OF THE IRRADIATED SPOT AND FRACTURE EDGE OF SAMPLE 4.

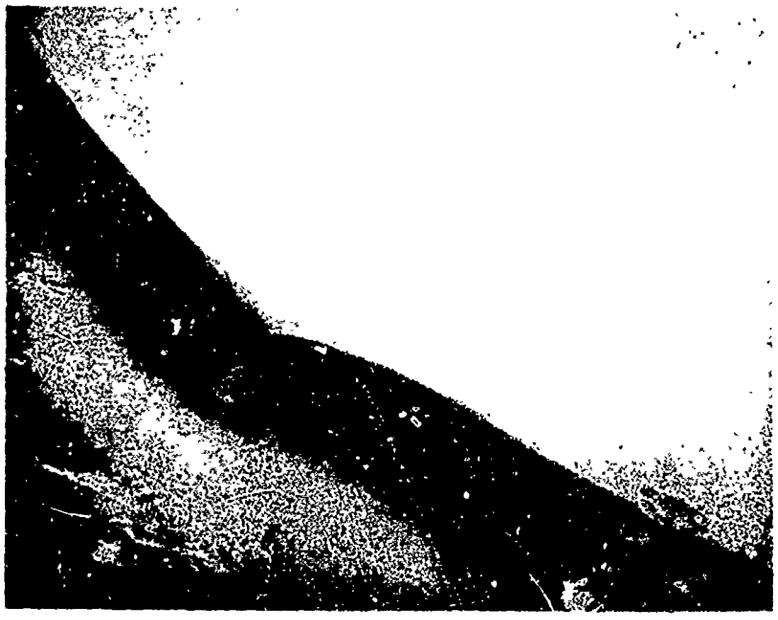

FIGURE 4-2. A SCANNING ELECTRON MICROGRAPH AT 61X AND 60 DEGREES.

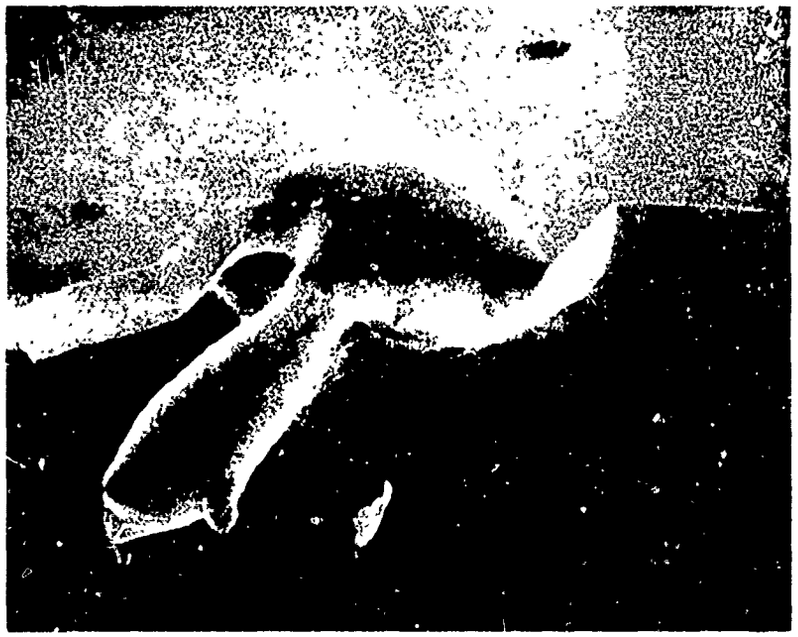

FIGURE 5-1. A SCANNING ELECTRON MICROGRAPH OF THE IRRADIATED SPOT AND FRACTURE EDGE OF SAMPLE 5 AT 60X AND 45 DEGREES.

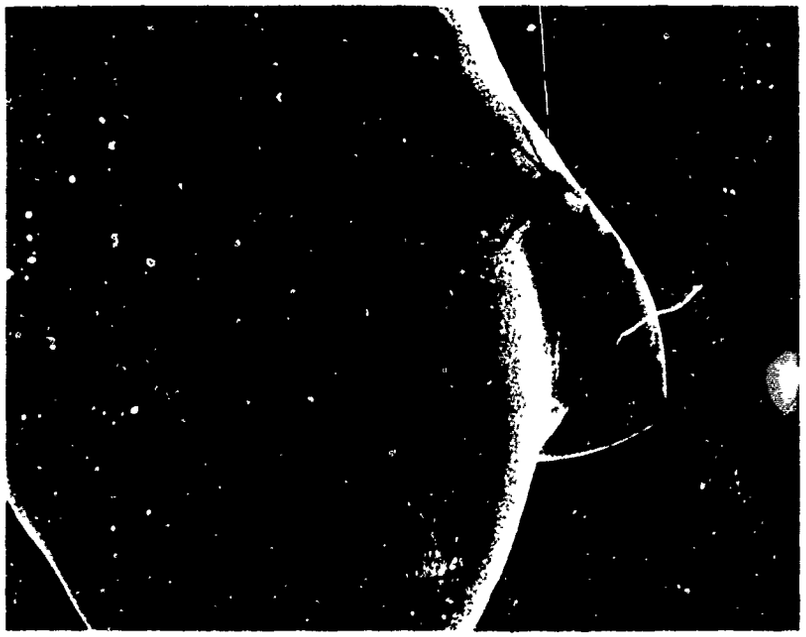

FIGURE 5-2. A SCANNING ELECTRON MICROGRAPH OF PART OF THE EXTRUDED MATERIAL AT 300X AND 45 DEGREES.

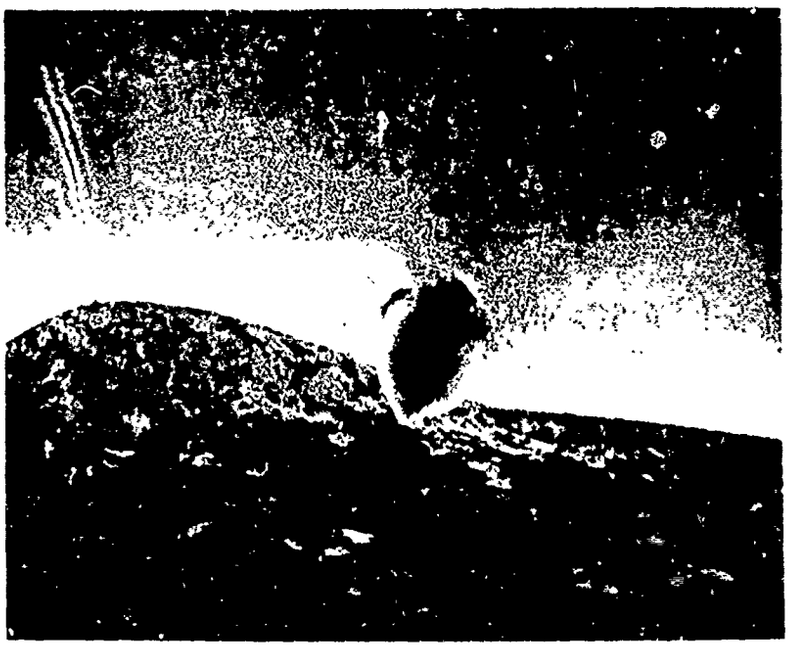

FIGURE 5-3. A SCANNING ELECTRON MICROGRAPH AT 600X AND 45 DEGREES OF PART OF THE EXTRUDED MATERIAL OF SAMPLE 5.

red. No evidence of surface modification was apparent on either front or rear surface, but there were several discolored regions visible on both the front and back surfaces. This sample was examined by infrared transmission spectroscopy, and the surface discoloration region exhibited an increased absorption at 9.3 micrometers, characteristic of a SiO_2 absorption band.

One sample from each of the two sets was studied by electron spin resonance. No significant differences were observed between the unirradiated and irradiated samples. A Laue photograph of sample 1 after irradiation revealed some slight misorientation of a small amount of crystalline material superimposed on the basic diffraction symmetry pattern characteristic of (111) silicon.

DISCUSSION

Based on the characteristic features observed on the group of silicon samples examined, four fundamental phenomena can be distinguished: stress relief, thermal etching, melting and catastrophic surface modification.

Stress relief is demonstrated in every thin sample by two features. Slip traces observed at the 120° angles characteristic of the (111) plane in silicon result from the translation of atomic layers in an attempt to relieve stress in the sample. Previous work on semiconductors irradiated by shorter wavelength lasers illustrated the formation of symmetry-defined patterns, with evidence of cracks following crystallographic directions.[26,27] The generation of slip lines in germanium crystals due to thermal strain has been demonstrated.[28] The generation of cracks in every thin silicon sample also demonstrates the attempt to relieve stress, though the fracture results in a catastrophic surface modification. The crack runs from (or to) the nearest edge, yet does not follow any preferred crystallographic direction; it extends completely through the sample, though not in a vertical plane. When the crack enters the irradiated region, surface perturbation is more severe. The behavior of the material surrounding the crack indicates that the crack is formed early in the exposure period.

A second feature observed for nearly every sample is thermal etching of the surface. The trigonal etch pits in the outer perimeter band are characteristic of the loss of surface material, here interpreted as due to heating and consequent vaporization. Sample 2 manifests the tendency for etching to propagate along surface inhomogeneities, such as surface scratches. The perimeter band on sample 2 extends a great distance from the center of the irradiated region into the region perturbed by the crack and reaches the nearest sample edge. That this behavior is the result of inhomogeneity in sample irradiation cannot be discounted, especially in view of the existence of additional melted regions between the principal region and the near edge. However, the symmetry of the central damage region tends to discount this possibility, as does the observation that the etching has propagated towards a severely disturbed region of the surface. Greater surface material loss has been observed for unetched Ge surfaces than for carefully prepared surfaces irradiated by a ruby laser.[29] The disparity, however, cannot be resolved on the basis of the post-mortem examination of one sample. Suffice it to say that an outer region of selective sample loss is prevalent, and that it tends to be accentuated in areas of previously perturbed surface. Laser generated etching has been observed previously,[30] and preferential surface modification on defects has been observed for ruby laser irradiation of metals.[31]

The etching behavior is complemented by the more complete thermally generated material modification caused by melting. The rapid liberation (10^{-14} sec)[32] of the energy from the absorbing modes provides an intense, sudden source of localized heating. If 2% of the incident energy were absorbed by a cylindrical sector of the sample 1 mm in diameter and 0.25 mm thick, the average temperature rise in the sample region would be on the order of 3000°K (assuming a constant heat capacity with no melting and no dissipative mechanisms). The actual energy profile is Gaussian over the irradiated region, giving rise to an inhomogeneous temperature rise, as is demonstrated experimentally by different degrees of surface perturbation.

Surface features developed during the initial thermal etching period tend to disappear during continued irradiation. In the inner portion of the exposed region, a smoothed surface lying in the focal plane is indicated by the uniform reflectivity in the LMs. The gradation of the wormlike ridge and valley structure at the boundary between outer and inner regions plus the depression of the inner region indicates that an etching period preceded the melting phenomenon. Melting in the perimeter band is confined to the peaks of the etched features. This local softening of sharp surface delineations occurs as more heat is concentrated at these points, either because of increased absorption or decreased dissipation.

The growth of a peak outward from the irradiated sample surface is the most interesting change in the silicon. Most previous work has demonstrated preferential material loss in the region of most intense light, and crater formation, spallation, and gas-jet formation are common observations.[26,29,31,33,34] A similar protuberance has been observed in germanium irradiated by a pulsed ruby laser.[26] Self-focusing effects, the most prevalent cause of damage in laser glasses, are much smaller at 10.6 μm than for similar powers at shorter wavelengths. One possible mechanism for peak formation is based on a subsurface temperature greater than that at the surface, an explanation used previously to describe crater and protuberance formation.[29,31] The pressure buildup in the sample interior would then force the outer surface to distort and relieve the stress. Surface tension could be responsible for drawing more material into the center. The generation of a high subsurface temperature in materials which are not strong absorbers of incident radiation is not without precedent. Blow-off is caused by vaporization of interior sample material.[35] The heat dissipating mechanisms (especially radiation) available to the outer surface layers are greater than those in the interior of a thermal insulator. The nonlinear sample temperature then generates nonlinear absorption and the gradient may increase. This mechanism is dependent on sufficiently uniform absorption of light through part of the depth of the sample to permit the temperature gradient to develop with inner material hotter than the surface. With an absorption coefficient of 1/cm at 10.6 μm at room temperature, thin samples are uniformly irradiated as a function of depth. Once the outer surface softens, the center expands to produce a mound of material extending from the surface. Another reasonable mechanism is based on nonlinear expansion of the material. The smaller thermal conductivity and higher thermal expansion coefficients at higher temperatures allow the central region to expand faster than the periphery, thus generating the observed peak.[36] The lack of distinctive ESR results reinforces the conclusion that the changes are due to melting rather than abrupt modification of chemical and physical structure.

Several results indicate that the surface does not become fluid. First, all samples were mounted vertically, yet there is no indication of flow due to gravity. If melting were complete, no protrusion as observed would be formed unless frozen momentarily or the result of a steady, balanced outward pressure. The surface features such as the white line residue characteristic of the scratch on sample 2 would have become less distinct, and the concentric ripples observable around the peak would have been lost. Yet the melting was complete enough that surface scratch pits lost their identity and the fault formed in sample 2 has apparently partially resealed at the inner end. When sample 5 shattered, the material in the melt region was pulled out of shape by the exiting fragment. The most consistent conclusion is that there is a plastic softening of the surface, with hotter material immediately beneath. Classical thermal strain studies on germanium have shown plastic material flow and cracking on cooling.[28]

The fourth phenomenon which is characteristic of these silicon samples is abrupt surface deformation. This is illustrated by the nipple at the peak of the protrusions observed on several samples and especially the rugged surface surrounding it. If this peak were produced during the formation of the protrusion, the melted material would have smoother the rough surface features. Yet these features show the sharp character of the cracks formed outside the perimeter band. Evidently this pinnacle was formed at the end of the irradiation period, or after the laser is turned off. If the peak grew by a series of projections thrust from beneath the surface, the concentric ring behavior can be accounted for. This ring pattern was also observed for the protuberance formed on Ge by ruby laser radiation.[26] The peak would grow in steps by the periodic ejection of material from the surface and melting. However, a more likely mechanism is that these peaks are slowly formed from the softened material and that the nipple is ejected from the hot interior just as the laser irradiation is completed and the sample begins to cool. Only this mechanism can account for the rugged surrounding surface. The gray veins are probably unoxidized silicon freshly exposed from beneath the surface during the final stages of peak formation or on cooling. Cracks similar in appearance were noted in germanium, but did not have the smooth surface nature observed in the melted silicon.[26] These material inhomogeneities are all characteristic of abrupt material displacement, showing skewing of lines on two samples, vein formation, and irregular surface projection, and giving rise to a slight misorientation in the Laue experiment.

A reconstruction of the events modifying the nature of the irradiated silicon can be deduced from the surface features observed:

1) Preferential material loss through thermal etching.

2) Slip trace generation and crack formation.

3) Central region softening.

4) Peak formation.

5) Abrupt surface disturbance.

A detailed time-dependent mechanistic study will be initiated to verify this chronology, and to identify the mechanism for nipple formation and generation of the concentric rings.

INVESTIGATION OF A POSSIBLE PROTECTIVE MECHANISM

One possible means of insulating electronic components from damage by CO_2 laser radiation involves the use of molecular gases which are strong light absorbers at 10.6 μm. An in-depth examination of the coupled rates which attempt to restore the molecular system to equilibrium thus providing continued usefulness of the absorbing gas, is needed to establish the feasibility of such a technique. Previous calculations have ignored the molecular states of the system,[11,37-39] or have considered the molecular states without the coupled hydrodynamic properties.[40-42] The coupling of the molecular state equations with the conservation equations which govern energy transfer and molecular transport properties is the soundest approach to the complete solution of the problem.

Molecular gases which are strong absorbers of 10.6 μm radiation have been used successfully to modulate the output of CO_2 lasers. SF_6, the most widely used of these gases, has been used to passively Q-switch [43] and mode-lock CO_2 lasers,[44] and other phenomena such as bleaching,[45-47] self-induced transparency[48] and photon echoes[49,50] manifest the strong interaction of the laser with the gas. These properties are dependent on the molecular rate processes responsible for the restoration of equilibrium in a perturbed system. These rate processes have been studied experimentally in detail,[38,41,42,51,52] but the theoretical description of the simultaneous mechanisms has previously required approximations which allow examination of only one process at a time.[38,42] An in-depth examination of the coupled rates which attempt to restore the molecular system to equilibrium would provide sequential recovery results.

The fundamental equations which describe the gas system are simply the three conservation equations: mass, momentum and energy. In addition, there is a continuity equation for each of the chemical species present.[53] An expanded version of the species continuity concept allows one to write an equation of continuity for each molecular state present. For simplicity the SF_6 molecular system may be approximated as a three-level system; the ground vibrational state labelled 3, the vibrational state to which molecules are excited by the CO_2 laser (most commonly the v=1 state of the ν_3 vibrational mode 965 cm^{-1} above the ground state) labelled 1, and a state labelled 2 which represets the path of other excited molecular states. In this manner the following set of equations may be written describing the system:

$$\frac{DN_1}{Dt} = \frac{\partial N_1}{\partial t} + (\underset{\rightarrow}{v}\cdot\underset{\rightarrow}{\nabla}N_1) = -N_1\,(\underset{\rightarrow}{\nabla}\cdot\underset{\rightarrow}{v}) - \underset{\rightarrow}{\nabla}\cdot N_1\underset{\rightarrow}{V}_1 + K_1 \qquad (1)$$

$$\frac{DN_2}{Dt} = \frac{\partial N_2}{\partial t} + (\underset{\rightarrow}{v}\cdot\underset{\rightarrow}{\nabla}N_2) = -N_2\,(\underset{\rightarrow}{\nabla}\cdot\underset{\rightarrow}{v}) - \underset{\rightarrow}{\nabla}\cdot N_2\underset{\rightarrow}{V}_2 + K_2 \qquad (2)$$

$$\frac{DN_3}{Dt} = \frac{\partial N_3}{\partial t} + (\underset{\rightarrow}{v}\cdot\underset{\rightarrow}{\nabla}N_3) = -N_3\,(\underset{\rightarrow}{\nabla}\cdot\underset{\rightarrow}{v}) - \underset{\rightarrow}{\nabla}\cdot N_3\underset{\rightarrow}{V}_3 + K_3 \qquad (3)$$

$$\frac{D\rho}{Dt} = \frac{\partial \rho}{\partial t} + (\underset{\rightarrow}{v}\cdot\underset{\rightarrow}{\nabla}\rho) = -\rho\,(\underset{\rightarrow}{\nabla}\cdot\underset{\rightarrow}{v}) \qquad (4)$$

$$\frac{D\underset{\rightarrow}{v}}{Dt} = \frac{\partial \underset{\rightarrow}{v}}{\partial t} + (\underset{\rightarrow}{v}\cdot\underset{\rightarrow}{\nabla v}) = -\frac{1}{\rho}(\nabla\cdot\vec{\vec{P}}) \tag{5}$$

$$\frac{D\hat{U}}{Dt} = \frac{\partial \hat{U}}{\partial t} + (\underset{\rightarrow}{v}\cdot\underset{\rightarrow}{\nabla}\hat{U}) = -\frac{1}{\rho}(\underset{\rightarrow}{\nabla}\cdot\underset{\rightarrow}{q}) - \frac{1}{\rho}(\vec{\vec{P}}:\underset{\rightarrow}{\nabla}\underset{\rightarrow}{v}) \tag{6}$$

External force terms have been neglected. N_1, N_2, and N_3 are the number densities of type 1, 2, and 3 molecules, with $N_1 = N_1(\underset{\rightarrow}{r},t) = N_1^e + n_1(\underset{\rightarrow}{r},t)$. ρ is the total density, and ρ_n the total number density. $\underset{\rightarrow}{v}$ is the bulk fluid velocity, $\underset{\rightarrow}{V}_i$ the diffusion velocity of the ith species, and $K_i = K_i(\underset{\rightarrow}{r},t) = K_i^e + \hat{K}_i(\underset{\rightarrow}{r},t)$ are the rates of production of species i. $\vec{\vec{P}}$ is the pressure tensor, $\hat{U}$ the internal energy per gram and $\underset{\rightarrow}{q}$ the energy flux vector.

As an initial approach to solving the problem of the molecular rate processes, assume that the laser is Q-switched with a pulse duration which is very short compared with the relaxation time of any of the restoring rates of the system. Then the laser pulse may be approximated as a delta function in time used to perturb the system and prepare an initial state which will then decay toward some equilibrium. The three continuity equations and the conservation of mass equation together represent a set of only three independent equations. Elimination of (3), substitution of (4) in the other equations to eliminate $\underset{\rightarrow}{v}$, and conversion of the energy conservation equation to one which is a temperature change equation yield four equations which may be expanded to first order in the change variables to obtain:

$$\frac{\partial n_1}{\partial t} = \frac{N_1^e}{\rho_n^o}\frac{\partial \rho}{\partial t^n} + D\nabla^2 n_1 - x_1 D\nabla^2\rho_n + K_{21}^e n_2 + K_{31}^e n_3 - (K_{12}^e + K_{13}^e)n_1 + (g_{12}+g_{13})T \tag{7}$$

$$\frac{\partial n}{\partial t^2} = \frac{N_2^e}{\rho_n^o}\frac{\partial \rho}{\partial t^n} + D\nabla^2 n_2 - x_2 D\nabla^2\rho_n + K_{12}^e n_1 + K_{32}^e n_3 - (K_{21}^e + K_{23}^e)n_2 + (g_{23}-g_{12})T \tag{8}$$

$$\frac{\partial^2 \rho_n}{\partial t^2} = \frac{kT_e}{m}\nabla^2\rho_n + \frac{\rho_n^o k}{m}\nabla^2 T + \frac{i\mu}{3\rho_n^o m}\nabla^2\frac{\partial \rho_n}{\partial t} \tag{9}$$

$$\frac{\partial T}{\partial t} = \lambda\nabla^2 T + \frac{kT_e}{\rho C_v}\frac{\partial \rho_n}{\partial t} - E_1 n_1 - E_2 n_2 - E_3\rho_n - E_g T \tag{10}$$

D is the diffusion coefficient, x_i the mole fraction of species, i, μ the bulk viscosity coefficient, k Boltzmann's constant, T_e the ambient temperature, T the temperature change from the ambient, λ the thermal conductivity coefficient and C_v the heat capacity per gram.

$$q_{ij} = N_i^e E_{ij} K_{ij}^e / kT_e^2 \; ; \; E_1 = -(E_{12}K_{12}^e + E_{23}K_{32}^e + E_{13}(K_{13}^e + K_{31}^e))/\hat{C}_v$$

$$E_2 = -(E_{23}(K_{23}^e + K_{32}^e) + E_{13}K_{31}^e - E_{12}K_{21}^e)/\hat{C}_v$$

$$E_3 = (E_{13}K_{31}^e + E_{23}K_{32}^e)/\hat{C}_v \qquad E_g = (E_{12}g_{12} + E_{13}g_{13} + E_{23}g_{23})/\hat{C}_v$$

Assuming a solution of the form:

$$n_l(r,z,\theta,t) = \sum_j \sum_k \sum_l A_{jkl} e^{\gamma_{jkl} t} R_j(r) Z_k(z) \Theta_l(\theta),$$

where $R_j(r)$, $Z_k(z)$ and $\Theta_l(\theta)$ are the eigenfunctions of the operator ∇^2 defined for the space under consideration. This generates a fifth order characteristic equation which may be solved to obtain a set of five roots. Solution is done by computer, and typical results for the lowest order in j,k, and l for a simplified three-level system are shown in Table I and Figs. 6 through 9. Three of the roots are real and negative. The fastest rate corresponds well with the sum of terms representing the rate at which molecules are lost from state 1, and shows the linear dependence on pressure characteristic of binary collision processes. Another rate labelled rate 2 shows a linear pressure dependence at pressures above 1 torr, but at low pressures is dominated by the inverse pressure dependence of the diffusion term. This rate agrees very well with the terms which are responsible for the equilibration of the nonequilibrium vibrational temperature with the temperature of the translational degrees of freedom. The third real rate has the inverse pressure dependence typical of a transport property, and agrees well with the rate at which heat is lost by the system. Agreement of this term with the thermal diffusion coefficient is enhanced when the real SF_6 system is considered rather than the three-level approximation. The complex conjugate roots give a real part which exponentially damps the traveling acoustic wave generated in the gas and represented by the imaginary part of the complex roots.

These results prove very informative. They show the dangerous anomaly present in concerted efforts to use saturable gases as a means of protecting materials from laser damage. To prevent saturation of the molecular transition, molecules must be rapidly removed from the excited states, or rapidly added to the absorbing states. The equations show the rate of excited state depopulation as rate 1, and the rate of repopulation of the absorbing state as rate 2. Both of these processes have a linear pressure dependence above the diffusion region, so that at higher pressures molecules are more quickly returned to the states which absorb the incoming radiation.[41] This indicates that raising the SF_6 pressure makes the gas a more efficient absorber, an effect which is conveniently complemented by the increased absorption at higher pressures. Unfortunately, however, increasing gas pressure shows a markedly slower rate of heat dissipation, so that the gas temperature rise becomes a difficult problem as the gas pressure is raised.[38,42] Further, acoustic wave generation and dissipation become a serious problem at higher pressures.[42,54] These unfavorable effects negate the usefulness of high absorber pressure.

TABLE 1

The Five Decay Rate Solutions of The Characteristic Equation as a Function of Gas Pressure

PRESSURE (Torr)	RATE 1	SUM 1	RATE 2	SUM 2	RATE 3	SUM 3	REAL(RATE 4)	IMAG(RATE 4)
0.1	-14703.	-14496.	-4409.	-4409.	-3898.8	-3898.8	-1233.6	49653.
0.5	-54803.	-53566.	-3331.	-3332.	- 779.8	- 779.8	- 246.7	49668.
1.0	-108440.	-106367.	-5492.	-5495.	- 389.9	- 389.9	- 123.3	49669.
5.0	-540310.	-529963.	-25591.	-25604.	- 78.0	- 78.0	- 24.7	49669.
10.0	-1080500.	-1059926.	-51065.	-51208.	- 39.0	- 39.0	- 12.3	49669.
50.0	-5402300.	-5299730.	-255140.	-256040.	- 7.8	- 7.8	- 2.5	49669.

all rates are in sec^{-1}

SUM 1 = $K_{12}^e + K_{32}^e + D\beta^2 + K_{13}^e + K_{31}^e$

SUM 2 = $K_{23}^e + K_{32}^e + D\beta^2 + K_{13}^e + K_{31}^e$

SUM 3 = $\lambda\beta^2$

β^2 is the sum of the eigen values of ∇^2

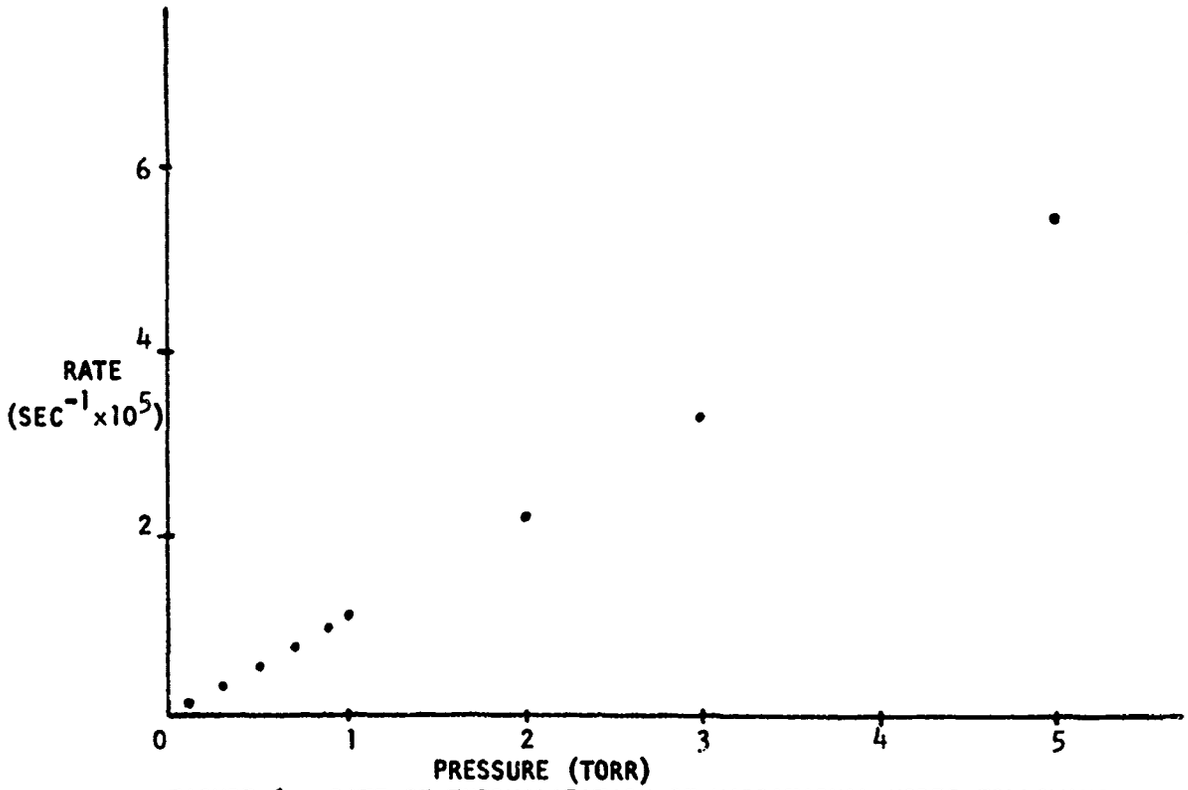

FIGURE 6. RATE OF THERMALIZATION OF VIBRATIONAL MODES FOLLOWING LASER EXCITATION VERSUS GAS PRESSURE IN TORR

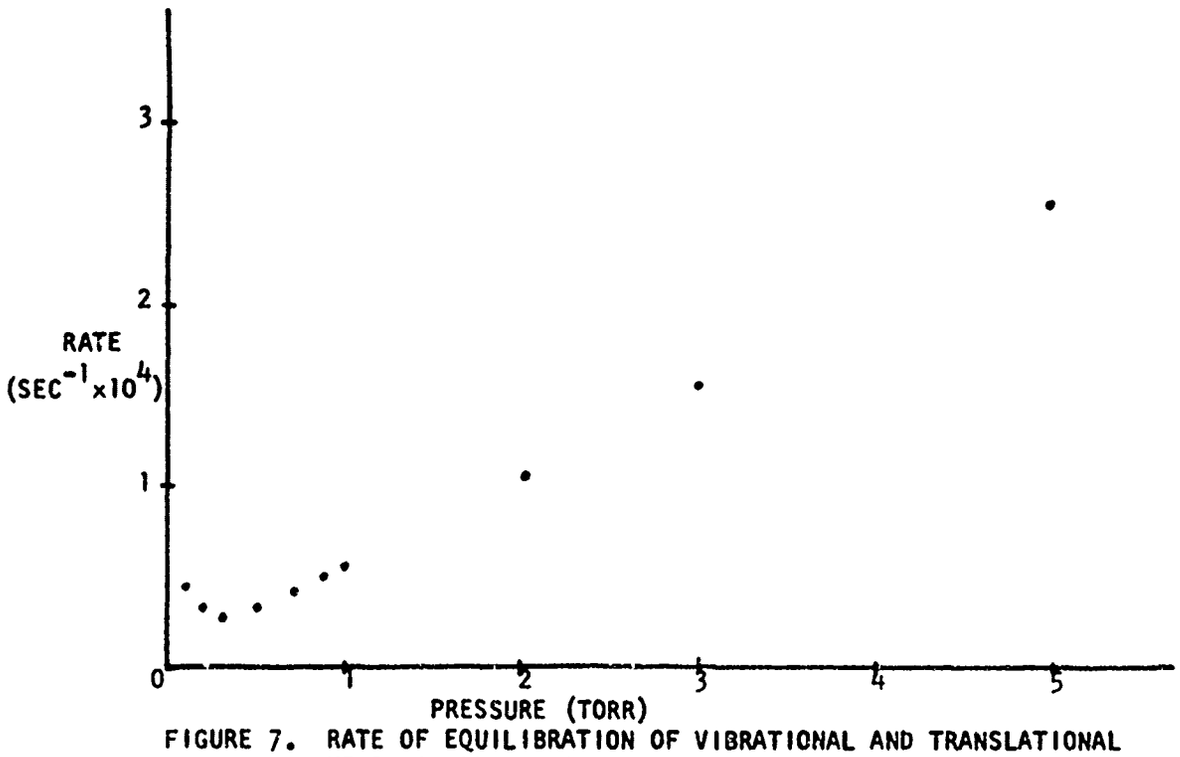

FIGURE 7. RATE OF EQUILIBRATION OF VIBRATIONAL AND TRANSLATIONAL TEMPERATURES VERSUS GAS PRESSURE IN TORR

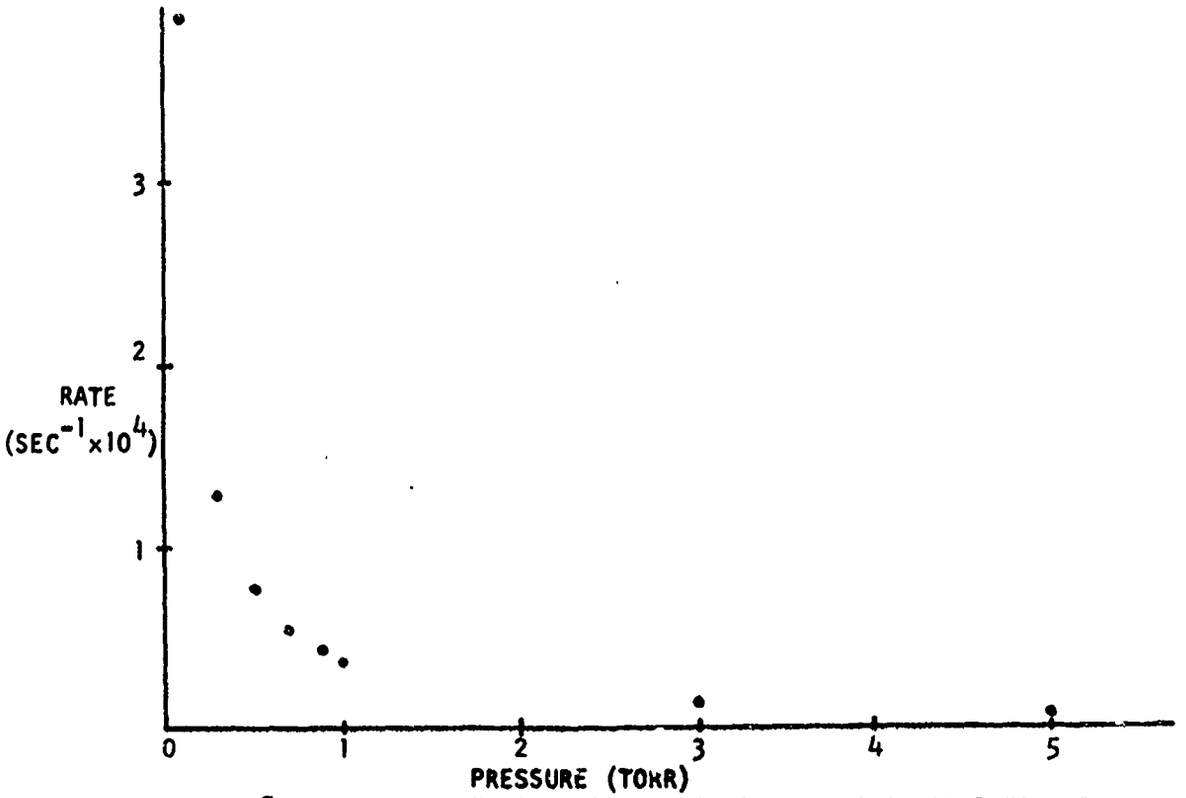

FIGURE 8. RATE OF THERMAL ENERGY TRANSPORT VERSUS GAS PRESSURE IN TORR

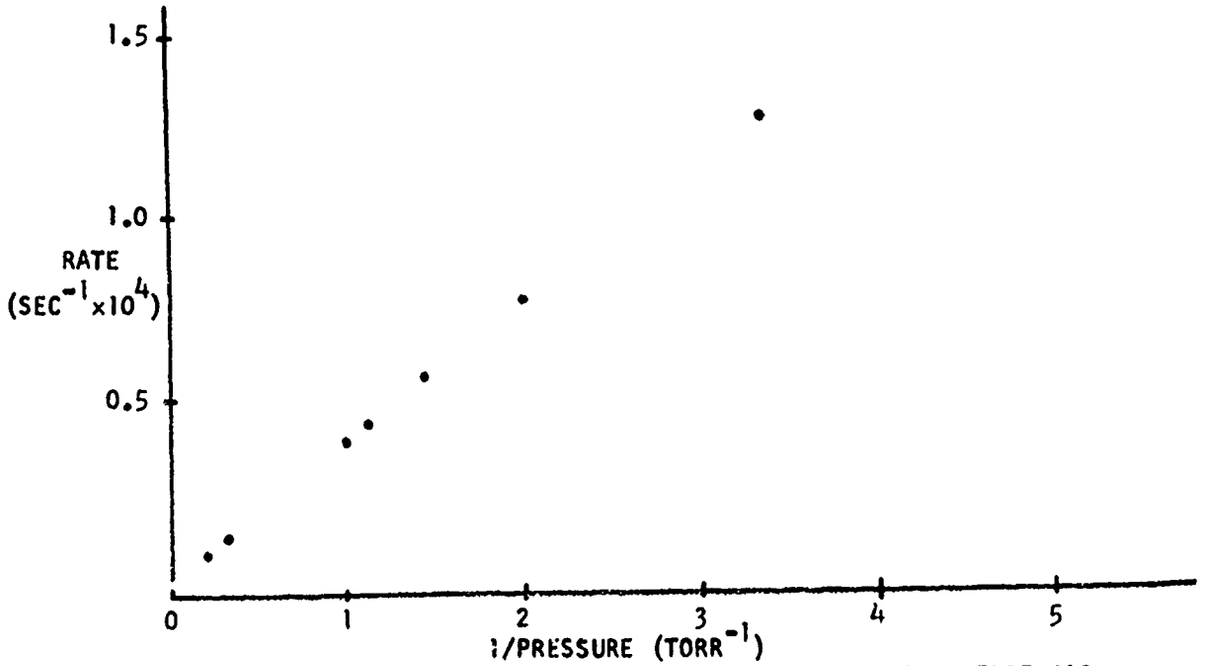

FIGURE 9. RATE OF THERMAL ENERGY TRANSPORT VERSUS INVERSE GAS PRESSURE IN RECIPROCAL TORR

Two possible remedies come immediately to mind. First, a thermal reservoir may be used to diminish the effects of heating and provide an increase in equilibration rate.[41,45] Second, the use of a bulk fluid flow to eliminate the effects of static absorber saturation is contemplated, in effect sweeping the laser energy from the components subject to damage. The results of these equations will be expanded to examine the effects of a constant input source in order to further investigate the capability of shielding electronic components. And specifically including the effects of a net flow by a constant fluid velocity perpendicular to the incoming laser beam will be investigated.

DISCUSSION OF SILICON PROTECTION

This initial effort barely scratches the surface of understanding the dominant interaction mechanisms operating during exposure of electronic components to laser radiation, let alone devises means of immunization. A preliminary examination of some proposals based on the experimental and theoretical information discussed in this report may prove illustrative. Admittedly, these initial mind-wanderings hardly describe well thought-out easily implemented alternatives, but merely an exposure of ideas.

First, three distinct types of materials which may be exposed to laser radiation may be differentiated.

Type I: Non-functioning components.

Type II: Components whose operation may be interrupted for periods of time to protect them from damage.

Type III: Elements which must continue operation.

An important subtype which could be labelled IIIa comprises those components which not only must continue operation, but whose fundamental purpose in operation is to monitor 10.6 μm radiation.

A similar categorization may be made of potential protective mechanisms. Passive measures are a general class of techniques which may include but are not limited to newly designed, nondestructive material, protective or ablative coatings, component arrays, and new materials which, though not immune to damage, are not rendered inoperative. Supplementing these alternatives are those which may be called active protective measures. One subset includes those which are always active, such as filters, mirrors, polarization selectors, moving slits, dynamic access programs or variable element arrays. The other subset includes active measures which must be made operational upon sensing the danger of potential laser damage. Sample mechanisms in this group could include mechanical shutters, electro-optical shutters or reflectors, gas dynamic absorbers and refractive index controls.

The experimental evidence for silicon samples demonstrates conclusively that the material perturbation mechanisms are heat related. The inability of the material to dispose of the induced thermal gradients is the primary cause of material modification. Thus, protective mechanisms for silicon would be based on one or more of three routes: A) limiting heating of the sample; B) dissipating heat more rapidly; or C) developing less heat-sensitive systems.

The objective of this project is not only to investigate the damage mechanisms induced by laser irradiation, but also to develop possible protective mechanisms which could prevent such damage. Based on the experimental and theoretical results obtained in this preliminary study, five possible means of immunizing electronic components will be discussed with reference to silicon irradiated at 10.6 μm.

1. Material design: The most direct approach would be to effect protection through material [illegible]. This is a passive measure which, if successful, would be applicable to all three types of use, and could follow any or all three of the immunization routes. The present results and those of other workers have indicated that surface preparation has significant influence on the nature and extent of surface damage.[29,31] The variation in nature of the damage as a function of sample size and thickness provides a second avenue of material control which may prove a viable mechanism for limiting damage. Use of a heat sink in conjunction with the operating material would provide a means of effecting protection under a B) type route, as would increasing the material thermal conductivity, especially on a local basis, through doping or mixing with favorable materials. Ironically one confusing result concerning the silicon experiments exists. There is no evidence that the observed material perturbation so alters the properties that catastrophic failure results. Obviously, controlled change such as that observed for samples 1-5 is preferable to complete destruction, depending on the specific type of usage and the necessary functioning characteristic of the material. The proposed study of amorphous semiconductors was prompted by the search for a material for which local chemical and physical property changes do not drastically modify functioning characteristics. One final note on material design: it is not necessarily an end in itself, but may be effectively combined with other proposed routes to ensure satisfying of requirements.

2. Coatings and shutters: This general class of protective mechanisms follows the A) and B) routes, and may be passive or active. Passive mechanisms could include reflective coatings such as a gold film which has been used to limit damage in other materials.[20] Ablative coating could be used to dissipate heat and thus reduce damage. Experimental studies of the damage to thin coatings have been initiated.[55] An additional group of protective means is activated shutters and reflectors such as Kerr cells and electro-optical shutters. These are activated to prevent damage to sensitive elements on sensing the danger of high-power radiation, much as the iris of the eye contracts or the eyelid closes. The fundamental consideration is the time the system has to respond before permanent damage is done. Future experimental work is designed to investigate the rate and mechanisms of the damage in order to facilitate the use of activated mechanisms of this type. Since the conversion of optical energy into heat is apparently very fast, the possibility exists that damage initiation occurs much faster than any device could operate. However, the experimental results indicate that damage in silicon samples occurs on a much longer time scale, and initiated devices may provide an acceptable means for protection of silicon components. Naturally, the effects of the laser radiation on the protective system then becomes a variable of paramount importance. This general protective mechanism would be unacceptable for Type IIIa materials, and for many applications of Type III materials.

3. Gas Flow: The difficulties involved in the use of static absorbers have been explored in the preceding section. This does not preclude the discovery of systems with molecular properties more amenable to this usage, or to the implementation of a flowing absorber system. This regeneration of the active medium may provide a combination system capable of transient protection of Type II and III materials, subject to the constraints discussed in the preceding paragraph, or it may afford a permanent screen to Type I and some Type II materials. These mechanisms are being investigated more fully on an experimental and theoretical level.

4. Dispersive Elements: The ability to deflect an unwanted radiation from the component to be protected would be a means for immunization. Classically, prisms and diffraction gratings have permitted discrimination of undesired wavelengths, without absorbing or reflecting the light. Such a device could be used to protect Types I-III materials, though it would not be effective for Type IIIa. An activated medium which produced controlled density fluctuations or in which the laser itself produced refractive index changes could be used to control the disposition of incoming beams. Unfortunately, these mechanisms show an ω^4 scattering dependence, and their feasibility in the IR seem marginal. However, the strong interaction of the laser beam with an absorbing medium may generate significant enough index of refraction changes that a dynamic medium would afford significant beam translation to protect the vulnerable component.

5. Pulse Coding: The problem of protection of Type IIIa materials is by far the most difficult. And the recovery of useful information from a large background of potentially damaging information is non-trivial. A possible approach is to so code the useful signal by a series of modulations that it may be recovered from the dc background by a series of narrow band filters. An alternative would be to periodically alter the polarization of the desired signal and discriminate against all but the coded signal on input. These mechanisms are not immunization techniques, but are means of information processing which require non-vulnerable detecting elements, as discussed under material design.

CONCLUSIONS

One ironical note may be added. Silicon was chosen for our first series of experiments because it possesses the desired well-characterized properties that would lend it to a detailed investigation of perturbation by laser irradiation. It was to be a foundation on which to build in future studies of more sophisticated systems. Yet it has shown resistance to drastic modification of properties when exposed at 10.6 μm. This does not mean that it is non-vulnerable, merely that it may also form a basis for designing more resistant materials. Future work will not only be devoted to a study of more complex materials, but also to detailed understanding of the mechanisms in silicon and the effects of parameter variation on the onset and nature of the damage.

ACKNOWLEDGMENTS

The authors gratefully acknowledge the contributions to this work by Messrs. T. AuCoin and M. Wade in sample preparation, P. Caplan for ESR studies, D. Eckart for X-ray Laue studies, W. Nye for early assistance on the project, Mrs. A. Dunlap for microscopy work, Dr. J. O'Connell for IR spectroscopy, and Drs. E. Poindexter, R. Buser, and J. Kohn for their guidance.

REFERENCES

1. Damage in Laser Glass, A.J. Glass and A.H. Guenther, Eds., ASTM Special Technical Publication 469, ASTM, Philadelphia (1969).

2. Damage in Laser Materials, A.J. Glass and A.H. Guenther, Eds., NBS Special Publication 341, U.S. Government Printing Office, Washington (1970).

3. Damage in Laser Materials, A.J. Glass and A.H. Guenther, Eds., NBS Special Publication 356, U.S. Government Printing Office, Washington (1971).

4. Effects of High Power Laser Radiation, J.F. Ready, Academic Press, New York (1971).

5. E.L. Kerr, Phys. Rev. A, 4, 1195 (1971).

6. See G.A. Henderson, AD-684581, U.S. Clearinghouse Fed. Sci. Tech. Information, (1968), bibliography.

7. J.T. Yardley, J. Chem. Phys 52, 3983 (1970).

8. R.J. Freiberg, IEEE J. Quant. Electronics JQE-6, 105 (1970); A.J. Beaulieu, Proc. IEEE, 226(1971).

9. W. B. Tiffany, R. Targ, J.D. Foster, Appl. Phys. Letters 15, 91 (1969); R. Targ and W.B. Tiffany, Appl. Phys. Letters 15, 302 (1969); A.S. Biriukov, A.P. Dronov, E.M. Koudriavtsev and N.N. Sobolev, IEEE J. Quant. Electronics JQE-7, 388 (1971).

10. For example: J.V.V. Kasper, J.H. Parker and G.C. Pimentel, J. Chem. Phys. 43, 1827 (1965); J.V.V. Kasper and G.C. Pimentel, Phys. Rev. Letters 14, 352 (1965); M.A. Pollack, Appl. Phys. Letters 9, 94 (1966).

11. P.R. Longaker and M.M. Litvac, J. Appl. Phys. 40, 4033 (1969).

12. F.G. Gebhardt and D.C. Smith, Appl. Phys. Letters 14, 52 (1969).

13. J.P. Gordon, H.J. Zeiger and C.H. Townes, Phys. Rev. 95, 282 (1954); C.H. Townes and A. Schawlow, Phys. Rev. 112, 1940 (1958).

14. T.H. Maiman, Phys. Rev. 123, 1145 (1961).

15. A. Javan, W.R. Bennett and D.R. Herriott, Phys. Rev. Letters 6, 106 (1961).

16. For example: R.K. Wilson and G. Busch, J. Chem. Phys. 56, 3655 (1972); N.V. Karlov, Y.B. Konev and A.M. Prokorov, Soviet Phys. JETP Letters 14, 117 (1971).

17. E. Yablonovitch, Appl. Phys. Letters 19, 495 (1971).

18. H. Pepin, K. Dick, J. Marineau and K. Parbhakar, Phys. Letters 38A, 203, (1972).

19. E.V. George, G. Bekefi and B. Ya'akobi, Phys. Fluids 14, 2708 (1971).

20. D. Poulsen, Appl. Optics 11, 949 (1972).

21. D.C. Hanna, B. Luther-Davies, H.N. Rutt, R.C. Smith and C.R. Stanley, IEEE J. Quant. Electronics, JQE-8, 317 (1972).

22. R.C. Smith and C.R. Stanley, Opt. Communications 2, 383 (1971).

23. A.M. Danishevskii, A.M. Kastal'skii, S.M. Ryvkin, I.D. Yarshetskii, Soviet Phys. JETP 31, 292 (1970).

24. A.F. Gibson and A.C. Walker, J. Phys. C, 4, 2209 (1971).

25. C.K.N. Patel and E.D. Shaw, Phys. Rev. Letters 24, 451 (1970).

26. M. Bertolotti, F. DePasquale, P. Marietti, D. Sette and G. Vitali, J. Appl. Phys. 38, 4088 (1967).

27. M. Birnbaum, J. Appl. Phys. 36, 3688 (1965).

28. P. Penning, Philips Research Reports 13, 79 (1958).

29. M. Bertolotti, L. Stagni, G. Vitali and L. Muzii, J. Appl. Phys 42, 5893 (1971).

30. R.R. Austin and A.H. Guenther, p. 137 of ref. 3.

31. K. Vogel and P. Backlund, J. Appl. Phys. 36, 3697 (1965).

32. J. Van Arsdale, ECOM R&D Technical Report 3023, (1968).

33. M. Birnbaum, Appl. Phys. Letters 10, 227 (1967).

34. A.A. Grinberg, R.F. Mekhtiev, S.M. Yyvkin, V.M. Salmanov and I.D. Yaroshetskii, Soviet Phys. Solid State 9, 1085 (1967).

35. For example: D.W. Harper, Brit. J. Appl. Phys. 16, 751 (1965); R.A. Miller and N.F. Borrelli, Appl. Optics 6, 164 (1967); B.F. Ponomarenko, V.I. Samoilov and P.I. Ulyakov, Soviet Phys. JETP 27, 415 (1968).

36. Compendium on High Power IR Laser Window Materials, C.S. Sahagian and C.A. Pitha, Air Force Cambridge Research Laboratory Special Report #135, (9 March 1972).

37. M.F. Goodman and E. Thiele, Phys. Rev. A,(3), 5, (1972).

38. R.D. Bates, Jr., G.W. Flynn, J.T. Knudtson, A.M. Ronn, J. Chem. Phys. 53, 3621 (1970).

39. P.V. Avizonis, C.B. Hogge, R.R. Butts and J.R. Kenemuth. Appl. Optics 11, 554 (1972).

40. J.T. Yardley and C.B. Moore, J. Chem. Phys 48, 14 (1967).

41. R.D. Bates, Jr., J.T. Knudtson, G.W. Flynn and A.M. Ronn, Chem. Phys. Letters 8, 103 (1971).

42. R.D. Bates, Jr., J.T. Knudtson, G.W. Flynn and A.M. Ronn, to be published, J. Chem. Phys., November 1972.

43. O.R. Wood and S.E. Schwarz, Appl. Phys. Letters 11, 88 (1967).

44. O.R. Wood and S.E. Schwarz, Appl. Phys. Letters 12, 263 (1968).

45. I. Burak, J.I. Steinfeld and D.G. Sutton, J. Quant. Spectry. Rad. Trans. 9, 959 (1969).

46. H. Brunet and M. Perez, Comptes Rendus B, 267, 1084 (1968).

47. O.R. Wood, P.L. Gordon and S.E. Schwarz, IEEE J. Quant. Electronics JQE-5, 502 (1969).

48. C.K.N. Patel and R.E. Slusher, Phys. Rev. Letters 19, 1019 (1967).

49. C.K.N. Patel and R.E. Slusher, Phys. Rev. Letters 20, 1087 (1968).

50. J.P. Gordon, C.H. Wang, C.K.N. Patel, R.E. Slusher and W.J. Tomlinson, Phys. Rev. 179, 294 (1969).

51. O.R. Wood and S.E. Schwarz, Appl. Phys. Letters 16, 518 (1970).

52. J.I. Steinfeld, I. Burak, D.G. Sutton and A.W. Nowak, J. Chem. Phys. 52, 5421 (1970).

53. Molecular Theory of Gases and Liquids, J.O. Hirshfelder, C.F. Curtiss and R.B. Bird, Wiley, New York (1954).

54. I. Burak, P. Houston, D.G. Sutton and J.I. Steinfeld, J. Chem. Phys. 53, 3632 (1970).

55. L.G. DeShazer and J.H. Parks, p. 124 of ref. 3.